ARTICLES

Journal of Semiconductors
(2019) 40, 022804
doi: 10.1088/1674-4926/40/2/022804
JOS

Thermally annealed gamma irradiated Ni/4H-SiC Schottky barrier diode characteristics

P. Vigneshwara Raja[1] and N. V. L. Narasimha Murty[2, †]

[1]Micro-Fabrication and Characterization Lab, School of Electrical Sciences, IIT Bhubaneswar, Odisha-752050, India

[2]Electrical Engineering, IIT Tirupati, Tirupati, Andhra Pradesh-517506, India

Abstract: Thermal annealing effects on gamma irradiated Ni/4H-SiC Schottky barrier diode (SBD) characteristics are analyzed over a wide range of temperatures (400–1100 °C). The annealing induced variations in the concentration of deep level traps in the SBDs are identified by thermally stimulated capacitance (TSCAP). A little decrease in the trap density at E_C – 0.63 eV and E_C – 1.13 eV is observed up to the annealing temperature of 600 °C. Whereas, a gamma induced trap at E_C – 0.89 eV disappeared after annealing at 500 °C, revealing that its concentration (< 10^{13} cm $^{-3}$) is reduced below the detection limit of the TSCAP technique. The electrical characteristics of irradiated SBDs are considerably changed at each annealing temperature. To understand the anomalous variations in the post-annealing characteristics, the interface state density distribution in the annealed SBDs is extracted. The electrical properties are improved at 400 °C due to the reduction in the interface trap density. However, from 500 °C, the electrical parameters are found to degrade with the annealing temperature because of the increase in the interface trap density. From the results, it is noted that the rectifying nature of the SBDs vanishes at or above 800 °C.

Key words: 4H-silicon carbide; Schottky barrier diode; thermal annealing; electrically active defects; thermally stimulated capacitance

Citation: P V Raja and N V L N Murty, Thermally annealed gamma irradiated Ni/4H-SiC Schottky barrier diode characteristics[J]. *J. Semicond.*, 2019, 40(2), 022804. http://doi.org/10.1088/1674-4926/40/2/022804

1. Introduction

Epitaxial 4H-silicon carbide (4H-SiC) Schottky barrier diode (SBD) detectors can be suitable for astronomy radiation imaging systems by considering their attractive features such as visible blindness, room temperature operation and radiation hardness[1–4]. In space environments, the detectors experience displacement damage due to exposure to high-energy gamma irradiation[4], thereby deteriorating the detector performance. So, studies on gamma irradiation induced displacement damage in the epitaxial 4H-SiC SBDs require special attention for such applications. To explore this, our earlier work[5] is targeted at analyzing the gamma irradiation effects on 4H-SiC SBDs at a high dose level of 100 Mrad. It is well known that thermal annealing can partially recover the radiation induced damage in the detectors[6, 7]; moreover, this study is important to extend the detector operational lifetime. Therefore, the current work focusses on investigating the annealing impacts on the gamma irradiated 4H-SiC SBDs.

Note that, Ni is a widely used metal for Schottky contact on n-type 4H-SiC epilayers because of its high work function and thermal stability[8–14]; and also, as-deposited Ti can create an Ohmic contact with a heavily doped (~10^{18} cm^{-3}) n-type 4H-SiC without any annealing process[15]. Considering these points, Ni/4H-SiC/(Ti/Au) SBDs on n-type epitaxial 4H-SiC (Ni Schottky contact and Ti based Ohmic contact) are used for the current study. In the literature, thermal annealing effects on non-irradiated 4H-SiC SBDs (i.e. changes in electrical characteristics and trap signatures) are extensively analyzed[11, 12, 16–29]. However, the annealing effects on gamma irradiated 4H-SiC SBD characteristics have not yet been examined. Hence, to understand the annealing impacts at various temperatures, thermal annealing studies are carried out on gamma irradiated (100 Mrad) Ni/4H-SiC SBDs over a wide range of temperatures (from 400 to 1100 °C). The thermal evolution of the deep level defects in the SBDs is investigated by an irreversible single shot capacitance transient technique called thermally stimulated capacitance (TSCAP) spectroscopy[5]. Furthermore, annealing induced changes in the electrical characteristics of the irradiated SBDs are analyzed.

2. Experiment

The Ni/4H-SiC SBDs were fabricated on n-type epitaxial 4H-SiC samples (30 μm epilayer with a doping concentration of 5 × 10^{14} cm^{-3}) from CREE Inc; the SBD fabrication details are discussed elsewhere[5, 30] and briefly discussed below. Upon the surface cleaning process, Ni (200 nm) was sputtered through a metal mask on the lightly doped epilayer (on the Si-face of 4H-SiC), which acts as a Schottky contact. Similarly, a sputtered Ti(50 nm)/Au(150 nm) bi-metal layer on the entire C-face of 4H-SiC (on highly doped ~10^{18} cm^{-3} substrate) was chosen for back Ohmic contact. It should be noted that both the top and back contacts of the SBDs were not annealed during the fabrication. The active area of the investigated SBDs is ~0.8 mm^2. The SBDs were irradiated with ^{60}Co-gamma rays up to a dose of 100 Mrad at UGC-DAE CSR, Kolkata centre; the irradiation information can be found elsewhere[5]. The TSCAP spectrum and electrical characteristics of the Ni/4H-SiC SBDs were measured before and after the gamma irradiation. The experimental procedure for acquiring the TSCAP spectrum is repor-

Correspondence to: N V L N Murty, nnmurty@iittp.ac.in
Received 9 AUGUST 2018; Revised 25 SEPTEMBER 2018.
©2019 Chinese Institute of Electronics

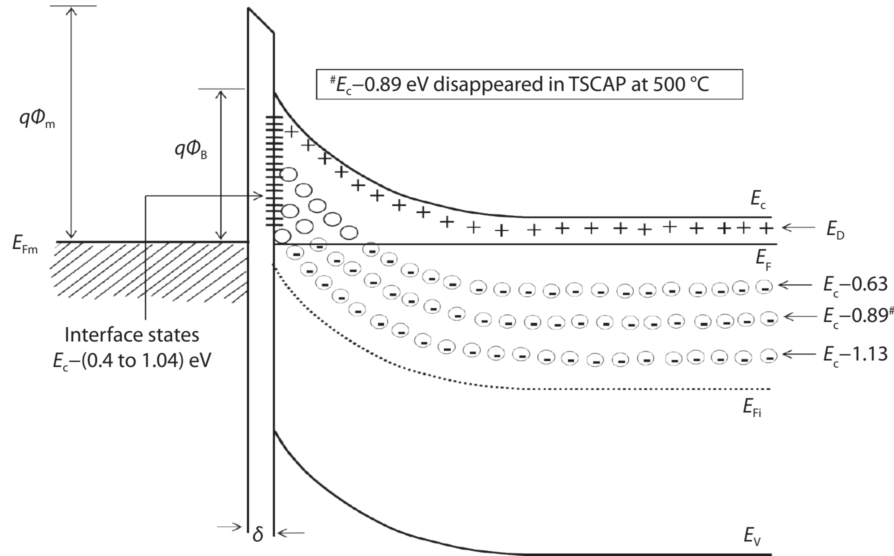

Fig. 1. The energy location of the bulk traps (E_C – 0.63 eV, E_C – 0.89 eV and E_C – 1.13 eV) and the interface states (E_C – 0.4 eV to E_C – 1.04 eV) in the energy band diagram of the Ni/4H-SiC SBDs.

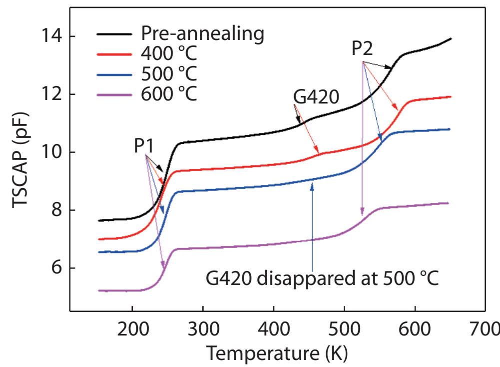

Fig. 2. (Color online) Changes in the TSCAP spectrum for gamma irradiated Ni/4H-SiC SBDs at different annealing temperatures from 400 to 600 °C.

ted in our earlier works[5,31]. In TSCAP measurements, upon cooling the sample to a low temperature of 150 K, the traps in the SBD were filled by injecting a forward current of 2 mA for 100 s. Thereafter, the sample temperature was increased up to 650 K at a heating rate of 0.12 K/s and subsequently the SBD capacitance versus temperature plot (i.e. TSCAP spectrum) was obtained at the reverse bias voltage of –40 V.

Thermal annealing of gamma irradiated SBDs was carried out by using a CARBOLITE GERO tube furnace (STF 16/450) from a temperature of 400 °C to a high temperature of 1100 °C with a step size of 100 °C in inert gas ambient. From the normal ambient conditions, the samples were loaded into the furnace to the desired annealing temperature. At each temperature, the samples were heated for 30 min duration in argon ambient. After annealing, the samples were unloaded and allowed to cool for some time in room ambience. Consequently, the TSCAP spectrum and electrical properties of the SBDs were measured after the heat treatments.

3. Results and discussion

Before discussing the annealing effects, it is important to know the gamma irradiation induced changes in the Ni/4H-SiC SBD characteristics at a dose of 100 Mrad are briefly described below[5]:

3.1. SBD characteristics before annealing

Two deep level bulk traps such as P1 (E_C – 0.63 eV, $Z_{1/2}$) and P2 (E_C – 1.13 eV, EH5) are detected in the non-irradiated SBDs with concentrations in the 10^{13} cm^{-3} range[5, 31]. After gamma irradiation, the trap density for P1 and P2 is increased by an order of magnitude (~10^{14} cm^{-3} range), along with the creation of a new trap G420 (E_C – 0.89 eV, $RD_{1/2}$) with a density of 3.8 × 10^{13} cm^{-3}[5]. The interface states in the non-irradiated SBDs are distributed over the energies of E_C – 0.4 eV to E_C – 1.04 eV, as determined from the forward I–V characteristics (discussed later)[11, 31, 32]. Surprisingly, no significant changes in the interface state density are found after irradiation. Fig. 1 shows the energy location of the bulk traps (P1, P2 and G420) and the interface states (E_C –0.4 eV to E_C – 1.04 eV) in the energy band diagram of the Ni/4H-SiC SBDs.

In non-irradiated SBDs, inhomogeneous[31, 33–35] Schottky barrier height (SBH) is identified at the Ni/4H-SiC interface with the two different SBHs (SBH1 = 1.18 eV, SBH2 = 1.29 eV) and ideality factors (n_1 = 1.32, n_2 = 1.88). In this condition, the current conduction preferentially occurs through the spatially localized low SBH regions at the Ni/4H–SiC interface, thereby deviating the electrical characteristics from the ideal case. This inhomogeneous nature is also observed in the irradiated SBDs. There are no considerable changes in the SBH (SBH1 = 1.2 eV, SBH2 = 1.3 eV) and ideality factor (n_1 = 1.33, n_2 = 1.9) values after irradiation. Hence, nonideal electrical properties are obtained for Ni/4H-SiC SBDs before and after irradiation. Moreover, a reduction in the forward current is noticed in the SBDs upon exposure to the gamma irradiation (because of the increased series resistance).

The effective doping concentration of 4H-SiC epilayer is decreased (from 5 × 10^{14} to 3.8 × 10^{14} cm^{-3}) after irradiation due to the compensation of the donor dopants by the irradiation produced acceptor-like deep level traps[5]. The frequency dependent C–V characteristics (capacitance increases with signal frequency) are observed in the SBDs before and after the irradiation. Most importantly, the reverse current is decreased

Table 1. Annealing induced changes in the electrical parameters and trap concentrations of the gamma irradiated Ni/4H-SiC SBDs.

Temp. (°C)	V_F at 1 mA (V)	SBH Φ_B (eV)	Ideality factor (n)	N_{eff} (10^{14} cm^{-3})	N_T (10^{14} cm^{-3})		
					P1	P2	G420
Preannealing	1.65	1.2 (SBH1), 1.3 (SBH2)	1.33 (n_1), 1.9 (n_2)	3.8	~1.8	~1.5	~0.38
400	1.7	1.4	1.32	3.16	~1.55	~1.35	~0.18
500	1.76	1.26	1.7	2.72	~1.4	~1.3	$
600	1.9	1.16	1.88	2	~1.3	~1.2	$
700	2	1.1	2.24	~1	*	*	*
800	3.75	1.01	8	#	*	*	*
900	12.4	0.98	12.6	#	*	*	*
1000	> 20	0.94	16.4	#	*	*	*
1100	> 20	0.88	24	#	*	*	*

$Trap G420 has disappeared from the TSCAP spectrum. #N_{eff} is not obtainable due to the nearly geometrical capacitance. *TSCAP is not measurable.

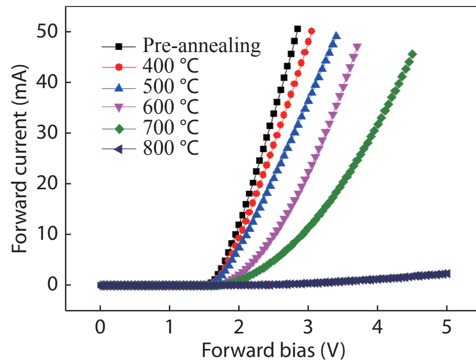

Fig. 3. (Color online) Annealing effects (400–800 °C) on forward current–voltage (I_F–V_F) characteristics of the gamma irradiated Ni/4H-SiC SBDs.

after gamma irradiation; the phenomenon behind this observation is reported in our earlier article[5].

3.2. SBD characteristics after annealing

Fig. 2 shows the TSCAP spectrum of the gamma irradiated Ni/4H-SiC SBDs at different annealing temperatures from 400 to 600 °C. The increasing TSCAP steps (P1, P2 and G420) in Fig. 2 reveal the electron traps in the SBD[5]. The mid-temperature ($T_{1/2}$) of the TSCAP step is extracted from the spectrum and the trap activation energy (E_T) is calculated by [5, 36]

$$E_T = kT_{1/2} \ln \frac{vkT_{1/2}}{q\left(E_T + 2kT_{1/2}\right)}, \tag{1}$$

where k is Boltzmann's constant, v is the escape frequency factor[5], and q is the elementary charge. The same energy location is identified for the traps P1 (E_C – 0.63 eV), G420 (E_C – 0.89 eV), P2 (E_C – 1.13 eV) in the annealed SBDs. The annealing induced changes in the trap concentration (N_T) are calculated from the TSCAP signal magnitude (step height) as per the following expression [5,36,37]

$$N_T = \frac{2\left(C_2 - C_1\right)}{C_1} N_d, \tag{2}$$

where C_1 is the capacitance at the step starting temperature, C_2 is the capacitance at the step ending temperature and N_d is the epilayer doping concentration. The trap concentrations determined at different annealing temperatures are summarized in Table 1. Note that, the TSCAP technique is very insensitive to the detection of interface states in the SBDs[5, 36, 37]. Moreover, the interface trap energies are expected to distribute continuously at the metal/semiconductor interface[38]; thus they possibly produce significantly longer TSCAP steps (broader spectrum in case of thermally stimulated current) based on their energy distribution range. Here, such a behavior is not observed in the TSCAP spectrum. Accordingly, it is considered that the deep levels P1, G420, and P2 belong to the bulk traps. From Fig. 2, it is noticed that the TSCAP spectrum shifts towards the downside after annealing (discussed later). A little decrease in the trap density for P1 and P2 is observed with the annealing temperature up to 600 °C (see Table 1), as similar to the annealing nature of non-irradiated 4H-SiC SBDs[31]. However, the trap concentrations for P1 and P2 are still in the range of 10^{14} cm^{-3}. On the other hand, the concentration of the trap G420 (RD$_{1/2}$) is minimized to half of its pre-annealing value (from 0.38×10^{14} to 0.18×10^{14} cm^{-3}) at 400 °C. Furthermore, the trap G420 has disappeared from the post-annealing TSCAP spectrum acquired at 500 °C (see Fig. 2), which reveals that the trap concentration for G420 is reduced (< 10^{13} cm^{-3}) below the detection limit of the TSCAP technique after the heat treatment at 500 °C. This result is contradictory to the observations of Dalibor *et al.*[39], where the RD$_{1/2}$ is thermally stable even at higher annealing temperatures (up to 1400 °C); but, their SBDs are not gamma irradiated. It is anticipated that the reduced trap density for G420 upon annealing at 500 °Cmay be advantageous in terms of minimizing the charge trapping effects in the real epitaxial 4H-SiC SBD detectors. The TSCAP spectra have not been acquired with the SBDs annealed ⩾ 700 °C, so thermal evolution of trap densities cannot be determined from 700 °C.

Fig. 3 displays the forward current-voltage (I_F–V_F) characteristics of the gamma irradiated Ni/4H-SiC SBDs for the annealing temperatures of 400 to 800 °C. The forward current is found to decrease with the annealing temperature. The variations in the forward voltage drop (V_F) at 1 mA, SBH, and ideality factor (n) of the SBDs are determined[12,31,38] at each annealing temperature and are summarized in Table 1. The changes in the I_F–V_F characteristics (in semi-log scale) of the gamma irradiated SBDs before and after the annealing temperature of 400 °C are plotted in Fig. 4. Two linear regions are perceived in the pre-annealing curve, whereas a single linear region is noticed in the post-annealing plot at 400 °C. Therefore, the double SBH nature[31, 33–35] of the pre-annealed gamma-irradiated SBDs is eliminated after the annealing at 400 °C and the

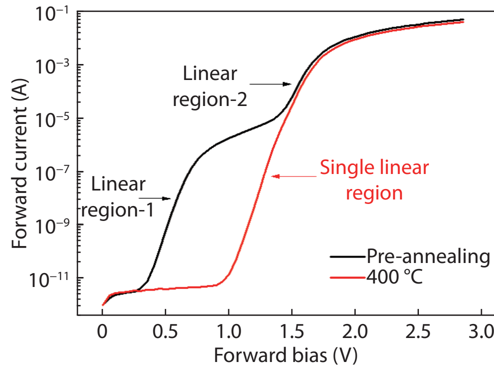

Fig. 4. (Color online) Changes in the I_F–V_F characteristics (in semi-log scale) of gamma irradiated Ni/4H-SiC SBDs before and after the annealing temperature of 400 °C.

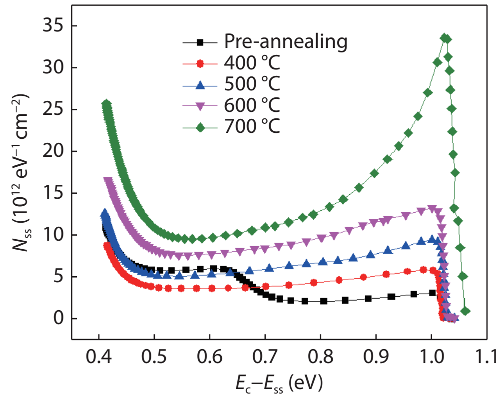

Fig. 5. (Color online) The distribution of interface state density (N_{SS}) as a function of E_C–E_{SS} calculated from the forward I–V characteristics of annealed (400–700 °C) gamma irradiated Ni/4H-SiC SBDs.

stable SBH of 1.4 eV is also achieved. The forward voltage (V_F) drop at 1 mA is increased to 1.7 V at 400 °C due to the improvement in the SBH (which reduces the thermionic emission current[38]). Nonetheless, the increase in the V_F at 1 mA is identified (although SBH decreases, see Table 1) along with the degraded ideality factors from 500 °C. So, anomalous I_F–V_F characteristics are obtained starting from the temperature of 500 °C.

To understand the abnormal variations in the post-annealing characteristics, the interface state density (N_{SS}) distribution in the annealed SBDs is computed[11, 31, 32] from the forward I–V characteristics. In this calculation, the SBH (Φ_B) is considered as bias-dependent and subsequently the effective SBH (Φ_{eff}) is evaluated by[11, 31, 32]

$$\Phi_{eff} = \Phi_B + \left(1 - \frac{1}{n(V_F)}\right) V_F, \quad (3)$$

where V_F is the forward voltage and the bias-dependent ideality factor $n(V_F)$ is expressed by[11,31,32]

$$n(V_F) = \frac{qV_F}{kT \ln(I_F/I_S)}, \quad (4)$$

where I_F is the forward current and I_S is the reverse saturation current. The interface trap density (N_{SS}) in equilibrium with the semiconductor can be written as[11, 31, 32]

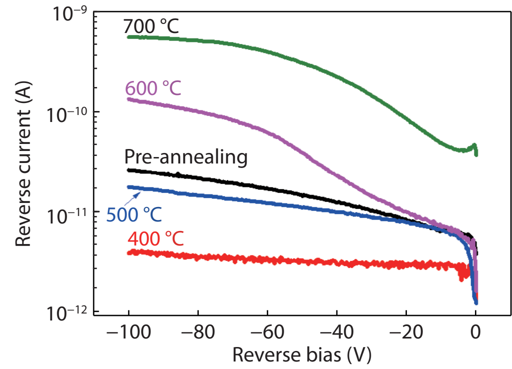

Fig. 6. (Color online) Annealing (400–700 °C) induced changes in the reverse current–voltage (I_R–V_R) characteristics of the gamma irradiated Ni/4H-SiC SBDs.

$$N_{SS} = \frac{1}{q}\left\{\frac{\varepsilon_i}{\delta}\left[n(V_F) - 1\right] - \frac{\varepsilon_S}{W}\right\}, \quad (5)$$

where ε_i is the interfacial oxide permittivity, δ is the oxide layer thickness identified from the high-frequency (1 MHz) C–V, ε_S is the permittivity of 4H-SiC, and W is the depletion region thickness estimated from the ($1/C^2$)–V properties at 1 MHz. The energy position of the interface states (E_{SS}) in n-type semiconductor is located with respect to the conduction band bottom (E_C), as given by[11, 31, 32]

$$E_C - E_{SS} = q(\Phi_{eff} - V_F). \quad (6)$$

Fig. 5 depicts the distribution profile of the interface state density (N_{SS}) as a function of E_C – E_{SS} for the annealed (400 – 700 °C) SBDs. Like non-irradiated 4H-SiC SBDs[11, 31, 32], exponential increase in the N_{SS} is noticed towards the conduction band edge for the annealed SBDs. The N_{SS} is significantly reduced in the energy range of E_C – 0.4 eV to E_C – 0.63 eV after the heat treatment at 400 °C. Thus, the observed enhancement in the SBH at 400 °C reveals that the interface states responsible for the dual SBH nature of pre-annealed SBDs is almost removed at 400 °C. In contrast, from 500 °C, the N_{SS} is found to rise with the annealing temperature. At 700 °C, the N_{SS} is dramatically increased to 3.35 × 10^{13} eV^{-1} cm^{-2} (at E_C – 1.0 eV) and 2.57 × 10^{13} eV^{-1} cm^{-2} (E_C – 0.4 eV) from the values at 500 °C of 4 × 10^{12} and 8.7 × 10^{12} eV^{-1} cm^{-2}. It is worth recalling that the trap G420 has disappeared from the post-annealing TSCAP at 500 °C and no significant modifications in the trap concentration for P1 and P2 are noted up to 600 °C. So, the reduction in the trap density of G420 (< 10^{13} cm^{-3}) at 500 °C has no effect on the electrical characteristics of the SBDs. As a result, the irregular changes in the I_F–V_F characteristics noticed from 500 °C are ascribed to the annealing induced increase in the N_{SS}.

The annealing (400–700 °C) induced changes in the reverse current–voltage (I_R–V_R) characteristics of the gamma irradiated Ni/4H-SiC SBDs are shown in Fig. 6. A substantial reduction in the reverse current is noticed at 400 °C due to the improvement in the SBH. Overall, the electrical parameters are improved upon the heat treatment at 400 °C, similar to the non-irradiated Ni/4H-SiC SBDs[11, 12, 31] (with Ti based Ohmic contact). However, beginning from the temperature of 500 °C, the reverse current is found to rise with the annealing due to the degraded SBH and the increased N_{SS}. So, the reverse I–V characteristics of the gamma irradiated SBDs deteriorate on or above

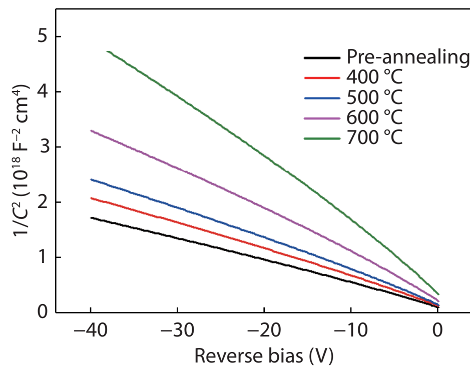

Fig. 7. (Color online) $(1/C^2)$–V characteristics at 1 MHz of gamma irradiated Ni/4H-SiC SBDs after heat treatments (400–700 °C).

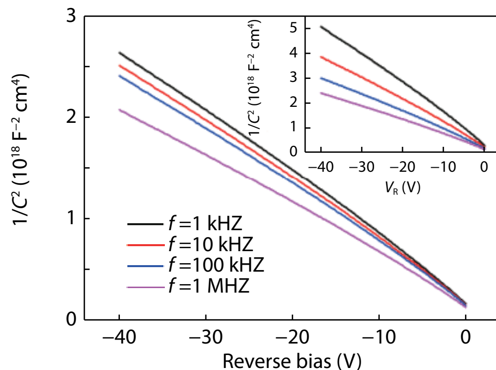

Fig. 8. (Color online) $(1/C^2)$–V characteristics at different signal frequencies (1 kHz–1 MHz) of the gamma irradiated Ni/4H-SiC SBDs at the annealing temperatures 400 and 500 °C (shown in inset).

500 °C as analogous to the forward I–V properties. These results suggest that a number of new interface traps are created after annealing ⩾ 500 °C and they again form an inhomogeneous Ni/4H-SiC Schottky barrier interface, thereby decreasing the SBH. Accordingly, the reverse current conduction may take place via the spatially localized low SBH section and hence the reverse current increases from 500 °C.

Fig. 7 shows the $(1/C^2)$–V characteristics at 1 MHz of the gamma irradiated Ni/4H-SiC SBDs after the heat treatments (400–700 °C). It is noticed that $1/C^2$ increases (capacitance decreases) with the annealing temperature. Hence, the annealing induced decrease in the capacitance is the reason for the downward movement of the post-annealing TSCAP spectrum seen in Fig. 2. The $(1/C^2)$–V characteristics at different signal frequencies (1 kHz to 1 MHz) for the SBDs at the annealing temperatures 400 and 500 °C are shown in Fig. 8 and in the inset. Similar to the pre-annealing case, frequency dependent $(1/C^2)$–V characteristics are obtained at 400 °C. It should be noted that the computed[31, 40] thermal emission time constant (≫1 ms) of the bulk traps P1, P2 and G420 is much higher than the C–V measurement time at the lowest signal frequency of 1 kHz. Therefore, the observed frequency dependence is not due to the bulk traps; it might be caused by the charge states at the Ni/4H-SiC interface. According to the calculated thermal emission time constant of the interface traps[31, 40], it is estimated that the interface traps located between the energies viz. E_C–0.4 eV to E_C–0.515 eV can affect the C–V measurements at the frequency of 1 kHz and the interface traps near to the energy E_C–0.4 eV can include their contribution to the measured capacitance up to 100 kHz. Thus, the frequency dependent

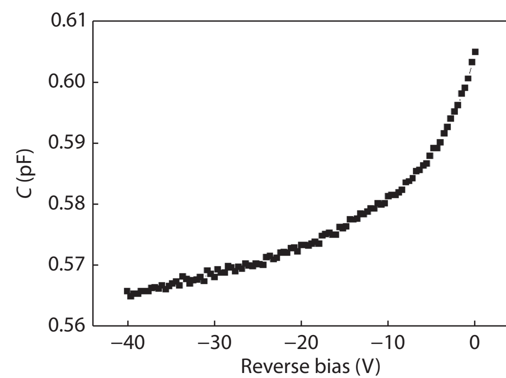

Fig. 9. Typical C–V characteristics (in diode geometrical capacitance range) obtained at all signal frequencies (1 kHz to 1 MHz) of the gamma irradiated Ni/4H-SiC SBDs for the annealing temperatures ⩾ 800 °C.

C–V characteristics may be produced by the interface trap energies E_C–0.4 eV to E_C–0.515 eV.

The decrease in the $1/C^2$ viewed in Fig. 8 with the signal frequency indicates the presence of acceptor-like interface traps in the SBDs. As a result, including the contribution of acceptor-like interface traps, reduced capacitance value (increased $1/C^2$) is obtained at low signal frequencies. Consequently, the measured capacitance increases with the signal frequency, as noted from Fig. 8. To minimize the interface state's charge contribution, the annealing induced changes in the effective doping concentration are evaluated from the $(1/C^2)$ $-V$ characteristics at the high signal frequency of 1 MHz. It is identified from Fig. 7 that the effective doping concentration is found to decrease with the annealing temperature (see Table 1). The effective doping concentration is reduced to 3.16×10^{14} cm^{-3} at 400 °C. Since the concentration of the deep level defects is not increased after the annealing, the donor concentration in the 4H-SiC epilayer must not be affected by them. In fact, the effective doping concentration is underestimated after annealing due to the contribution of the acceptor-like interface states. Strong frequency dependent $(1/C^2)$–V characteristics perceived at 500 °C (see the inset of Fig. 8) also reveal the creation of the acceptor-like interface traps after annealing. Accordingly, the effective doping concentration at 700 °C is undervalued (~1×10^{14} cm^{-3}) by about four times its pre-annealing value.

Fig. 9 shows the C–V characteristics of the gamma irradiated Ni/4H-SiC SBDs for the heat treatments ⩾ 800 °C (up to 1100 °C). A minor variation in the capacitance is noted with the bias voltage. However, these capacitance values are in the order of the diode geometrical capacitance[31, 38], by considering the SBD active area (~0.8 mm^2) and the total thickness (~395 μm) including the substrate and the epitaxial layer. Moreover, similar C–V properties are noticed at all the signal frequencies (1 kHz to 1 MHz). Because of these peculiar C–V characteristics, the changes in the effective doping concentration are not obtainable from 800 °C.

Fig. 10 shows the typical I–V characteristics (−20 to 20 V) of the gamma irradiated Ni/4H-SiC SBDs at the annealing temperature of 950 °C. Very low forward current (0.54 nA at 5 V and 1.74 μA at 10 V) is obtained at 950 °C. Furthermore, undesirable electrical parameters (V_F at 1 mA > ~4 V, SBH < 1 eV, and n > 8) are identified for the SBDs annealed ⩾ 800 °C (see Table 1). So, the I–V and C–V characteristics state that the rectify-

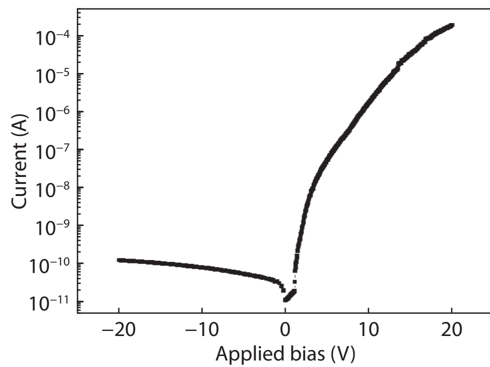

Fig. 10. Typical *I*–*V* characteristics (–20 to 20 V) of the gamma irradiated Ni/4H-SiC SBDs at the annealing temperature of 950 °C.

ing properties of the SBDs have vanished from the annealing temperature of 800 °C. It is reported[41–43] that the Ni Schottky contact on n-type 4H-SiC epilayers can change into an Ohmic contact around the annealing temperature of 950 °C. Here, Ohmic nature is not found in the *I*–*V* characteristics (asymmetrical *I*–*V* in Fig. 10) at 950 °C (even up to 1100 °C). Generally, the Ni/4H-SiC Schottky contact is expected to improve after the annealing temperatures of 500–700 °C due to the creation of nickel silicide at the interface[8, 40, 44, 45]. In this work, considerable deterioration in the electrical characteristics is observed from the temperature of 500 °C. As a result, the reason for the disappearance of the SBD rectifying behavior may be associated with the deterioration in the back contact properties (Ti/Au bilayer with 4H-SiC substrate) at elevated temperatures. From the work of Kim *et al.*[46], it is noted that 800 °C is not the eutectic temperature for Ti/4H-SiC interface. However, it is clear that the rectifying property of the Ni/4H-SiC SBDs (with Ti based Ohmic contact) has vanished from 800 °C. Studies are underway to understand the physical mechanism responsible for the disappearance of the SBD rectification at ~800 °C.

4. Conclusion

Thermal annealing induced changes in the gamma irradiated Ni/4H-SiC SBD properties are investigated over a wide range of temperatures 400–1100 °C. The concentration of the trap at E_C–0.89 eV is reduced (< 10^{13} cm^{-3}) below the detection limit of the TSCAP technique at the annealing temperature of 500 °C; the reduced trap density for G420 upon annealing at 500 °C may be beneficial in terms of minimizing the charge trapping effects in the real epitaxial 4H-SiC SBD detectors. On the other hand, no considerable changes in the trap density for E_C–0.63 eV and E_C–1.13 eV are identified up to 600 °C. Like non-irradiated Ni/4H-SiC SBDs (with Ti based Ohmic contact), the electrical characteristics are improved at 400 °C with the disappearance of dual SBH nature and the reduction in the interface trap density. Hence, the optimum annealing temperature for these kinds of Ni/4H-SiC SBD structures is ~400 °C. Nevertheless, from 500 °C, the electrical characteristics are found to degrade with the annealing temperature due to the increase in the interface state density. Reasonable electrical properties are noted up to 600 °C and finally, the SBD rectification has disappeared from 800 °C.

Acknowledgment

The authors would like to thank CSIR-CEERI for providing facilities for SBD fabrication. We also would like to thank Dr. Abhijit Saha, UGC-DAE CSR, Kolkata, for the gamma irradiation of SBDs.

References

[1] Xin X, Yan F, Koeth T W, et al. Demonstration of the first 4H-SiC EUV detector with large detection area. NASA Technical Report Server, 2005.[online]. Available: https://ntrs.nasa.gov/search.jsp?R=20090022809
[2] Xin X, Yan F, Koeth T W, et al. Demonstration of 4H-SiC UV single photon counting avalanche photodiode. Electron Lett, 2005, 41(4), 212
[3] Lees J E, Bassford D J, Bunce E J, et al. Silicon carbide X-ray detectors for planetary exploration. Nucl Instr Meth Phys Res A, 2009, 604(1/2), 174
[4] Huber M C E, Pauluhn A, Culhane J L, et al. Observing photons in space: a guide to experimental space astronomy. New York: Springer, 2013
[5] Raja P V, Murty N V L N. Thermally stimulated capacitance in gamma irradiated epitaxial 4H-SiC schottky barrier diodes. J Appl Phys, 2018, 123(16), 161536
[6] Castaldini A, Cavallini A, Rigutti L, et al. Low temperature annealing of electron irradiation induced defects in 4H-SiC. Appl Phys Lett, 2004, 85(17), 3780
[7] Iwamoto N, Johnson B C, Ohshima T, et al. Annealing effects on charge collection efficiency of an electron-irradiated 4H-SiC particle detector. 10th international workshop on radiation effects on semiconductor devices for space applications (RASEDA-10), 2013, 42
[8] Zetterling C M, Lee S K, Ostling M. Schottky and ohmic contacts to SiC, in Process technology for silicon carbide devices. London: INSPEC IET, 2002: 111
[9] Roccaforte F, La Via F, Baeri A, et al. Structural and electrical properties of Ni/Ti schottky contacts on silicon carbide upon thermal annealing. J Appl Phys, 2004, 96(8), 4313
[10] Strel'chuk A M, Davydov A V, Tringe J, et al. Characteristics of He+-irradiated Ni schottky diodes based on 4H-SiC epilayer grown by sublimation. Phys Status Solidi C, 2009, 6(12), 2876
[11] Gupta S K, Azam A, Akhtar J. Improved electrical parameters of vacuum annealed Ni/4H-SiC (0001) schottky barrier diode. Physica B, 2011, 406(15/16), 3030
[12] Gupta S K, Pradhan N, Shekhar C, et al. Design, fabrication, and characterization of Ni/4H-SiC (0001) schottky diodes array equipped with field plate and floating guard ring edge termination structures. IEEE Trans Semicond Manuf, 2012, 25(4), 664
[13] Kumar V, Kaminski N, Maan A S, et al. Capacitance roll-off and frequency-dispersion capacitance-conductance phenomena in field plate and guard ring edge-terminated Ni/SiO_2/4H-nSiC schottky barrier diodes. Phys Status Solidi A, 2016, 213(1), 193
[14] Kumar V, Maan A S, Akhtar J. Tailoring surface and electrical properties of Ni/4H-nSiC schottky barrier diodes via selective swift heavy ion irradiation. Phys Status Solidi A, 2018, 215(5), 1700555
[15] Huang L, Liu B, Zhu Q, et al. Low resistance Ti Ohmic contacts to 4H-SiC by reducing barrier heights without high temperature annealing. J Appl Phys, 2012, 100(26), 263503
[16] Kcstle A, Wilks S P, Dunstan P R, et al. Improved Ni/SiC Schottky diode formation. Electron Lett, 2000, 36(3), 267
[17] Sochacki M, Szmidt J, Bakowski M, et al. Influence of annealing on reverse current of 4H-SiC schottky diodes. Diamond Relat Mater, 2002, 11(3-6), 1263
[18] Pérez R, Mestres N, Montserrat J, et al. Barrier inhomogeneities and electrical characteristics of Ni/Ti bilayer schottky contacts on 4H-SiC after high temperature treatments. Phys Status Solidi A, 2005, 202(4), 692
[19] Pe'rez R, Mestres N, Tournier D, et al. Ni/Ti ohmic and Schottky

contacts on 4H-SiC formed with a single thermal treatment. Diamond Relat Mater, 2005, 14(3-7), 1146

[20] Calcagno L, Ruggiero A, Roccaforte F, et al. Effects of annealing temperature on the degree of inhomogeneity of nickel-silicide/SiC schottky barrier. J Appl Phys, 2005, 98(2), 023713

[21] Oder T N, Martin P, Adedeji A V, et al. Improved schottky contacts on n-type 4H-SiC using ZrB_2 deposited at high temperatures. J Electron Mater, 2007, 36(7), 805

[22] Oder T N, Sung T L, Barlow M, et al. Improved Ni schottky contacts on n-type 4H-SiC using thermal processing. J Electron Mater, 2009, 38(6), 772

[23] Ramesha C K, Reddy V R. Influence of annealing temperature on the electrical and structural properties of palladium schottky contacts on n-type 4H-SiC. Superlattices Microstruct, 2014, 76, 55

[24] Han L C, Sun H J, Liu K A, et al. Annealing temperature influence on the degree of inhomogeneity of the schottky barrier in Ti/4H-SiC contacts. Chin Phys B, 2014, 23(12), 127302

[25] Pristavu G, Brezeanu G, Badila M, et al. A model to non-uniform Ni schottky contact on SiC annealed at elevated temperatures. Appl Phys Lett, 2015, 106(26), 261605

[26] Kyoung S, Jung E, Sung M Y. Post-annealing processes to improve inhomogeneity of schottky barrier height in Ti/Al 4H-SiC schottky barrier diode. Microelectron Eng, 2016, 154, 69

[27] Yun S B, Kim J H, Kang Y H, et al. Optimized annealing temperature of Ti/4H-SiC schottky barrier diode. J Nanosci Nanotechnol, 2017, 17(5), 3406

[28] Storasta L, Tsuchida H, Miyazawa T, et al. Enhanced annealing of the $Z_{1/2}$ defect in 4H-SiC epilayers. J Appl Phys, 2008, 103(1), 013705

[29] Mannan M A, Nguyen K V, Pak R O, et al. Deep levels in n-type 4H-silicon carbide epitaxial layers investigated by deep-level transient spectroscopy and isochronal annealing studies. IEEE Trans Nucl Sci, 2016, 63(2), 1083

[30] Raja P V, Akhtar J, Rao C V S, et al. Spectroscopic performance studies of 4H-SiC detectors for fusion alpha-particle diagnostics. Nucl Instrum Methods Phys Res A, 2017, 869, 118

[31] Raja P V, Murty N V L N. Thermal annealing studies in epitaxial 4H-SiC schottky barrier diodes over wide temperature range. Microelectron Reliab, 2018, 87, 213

[32] Sochacki M, Kolendo A, Szmidt J, et al. Properties of Pt/4H-SiC schottky diodes with interfacial layer at elevated temperatures. Solid State Electron, 2005, 49(4), 585

[33] Bhatnagar M, Baliga B J, Kirk H R, et al. Effect of surface inhomogeneities on the electrical characteristics of SiC Schottky contacts. IEEE Trans Electron Devices, 1996, 43(1), 150

[34] Defives D, Noblanc O, Dua C, et al. Barrier inhomogeneities and electrical characteristics of Ti/4H-SiC Schottky rectifiers. IEEE Trans Electron Devices, 1999, 46(3), 449

[35] Zhang Q, Sudarshan T S. The influence of high-temperature annealing on SiC Schottky diode characteristics. J Electron Mater, 2001, 30(11), 1466

[36] Lang D V. Space-charge spectroscopy in semiconductors. In: Thermally stimulated relaxation in solids. Berlin: Springer, 1979, 93

[37] Miller G L, Lang D V, Kimerling L C. Capacitance transient spectroscopy. Ann Rev Mater Sci, 1977, 7, 377

[38] Sze S M, Ng K K. Physics of semiconductor devices. New Jersey: John Wiley & Sons, 2007

[39] Dalibor T, Pensl G, Matsunami H, et al. Deep defect centers in silicon carbide monitored with deep level transient spectroscopy. Phys Status Solidi A, 1997, 162(1), 199

[40] Kimoto T, Cooper J A. Fundamentals of silicon carbide technology growth, characterization, devices, and applications. Singapore: John Wiley & Sons, 2014

[41] Han S Y, Kim K H, Kim J K, et al. Ohmic contact formation mechanism of Ni on n-type 4H-SiC. Appl Phys Lett, 2001, 79(12), 1816

[42] Han S Y, Lee J. Effect of interfacial reactions on electrical properties of Ni contacts on lightly doped n-type 4H-SiC. J Electrochem Soc, 2002, 149(3), G189

[43] Han S Y, Shin J, Lee B, et al. Microstructural interpretation of Ni ohmic contact on n-type 4H-SiC. J Vac Sci Technol B, 2002, 20(4), 1496

[44] Omar S U, Sudarshan T S, Rana T A, et al. Interface trap-induced nonideality in as-deposited Ni/4H-SiC schottky barrier diode. IEEE Trans Electron Devices, 2015, 62(2), 615

[45] Zhao J H, Sheng K, Lebron-Velilla R C. Silicon carbide Schottky barrier diode. Int J High Speed Electron, 2005, 15(4), 821

[46] Kim D H, Lee J H, Moon J H, et al. Improvement of the reverse characteristics of Ti/4H-SiC Schottky barrier diodes by thermal treatments. Solid State Phenom, 2007, 124-126, 105